

THE UNIVERSITY OF MICHIGAN  
COLLEGE OF ENGINEERING  
Department of Nuclear Engineering

Final Report - Part 2

ESR RESULTS OF ZnSe AND OTHER HEXAGONAL A<sub>II</sub>B<sub>VI</sub> COMPOUNDS

G. Hossein Azarbajejani

ORA Project 04385

under contract with:

NATIONAL SCIENCE FOUNDATION  
GRANT NO. G-15912  
WASHINGTON, D.C.

administered through:

OFFICE OF RESEARCH ADMINISTRATION      ANN ARBOR

June 1963

en sm  
UMR 20161

## TABLE OF CONTENTS

	Page
LIST OF TABLES	v
LIST OF FIGURES	vii
ABSTRACT	1
CHAPTER	
I. INTRODUCTION	1
II. RESULTS	3
A. Experimental	3
B. Theoretical	6
C. Determination of $g$ , $A$ , $D$ , $a$ , and $F$	21
III. DISCUSSION	23
REFERENCES	30



## LIST OF TABLES

Table	Page
I. Absorption Peak Positions (in gauss) of the Lines Designated in Figs. 1 and 2.	6
II. $Mn^{++}$ ESR Parameters in Hexagonal $A_{II}$ $B_{VI}$ Compounds.	23
III. Crystalline Parameters of $A_{II}$ $B_{VI}$ Compounds.	25



## LIST OF FIGURES

Figure	Page
1a-4a. ESR Spectra of $Mn^{++}$ in the Plane $(10\bar{1}0)$ of ZnSe. $\theta$ is the angle between c-axis and $\underline{H}$ .	4 4
1b-4b. ESR Spectra of $Mn^{++}$ in the Plane $(10\bar{1}0)$ of ZnSe. $\theta$ is the angle between c-axis and $\underline{H}$ . ( $M = -1/2 \rightarrow +1/2$ transitions; signal level is reduced by a factor of 3.)	5 5
5. Relative positions of the magnetic ( $\underline{H}$ Polar Axis) and Crystalline coordinate systems.	8
6. Change of the axis of quantization (z-axis) from $[100]$ to $[111]$ direction and the result of $C_2$ operation on xyz coordinate system.	10
7. Ideal hexagonal packing.	26
8. Schematic representation of surrounding ligands around the $Mn^{++}$ ion in ZnSe:Mn.	28

## ABSTRACT

ESR experiments on  $\text{ZnSe:Mn}^{++}$  have been carried out at room temperature with X-, Ku-, and K-band microwave spectrometers. Parameters  $g$  and  $A$  are isotropic, with values of  $2.0055 \pm 5$  and  $-61.2 \pm .5 \times 10^{-4} \text{ cm}^{-1}$  respectively. The following values were obtained for parameters  $D$ ,  $a$ , and  $F$ :  $D = 425.1 \times 10^{-4} \text{ cm}^{-1}$ ;  $a = 17.66 \times 10^{-4} \text{ cm}^{-1}$ ; and  $F = 6.61 \times 10^{-4} \text{ cm}^{-1}$ .

## I. INTRODUCTION

It was pointed out previously<sup>1,2</sup> that the Watanabe<sup>3</sup> theory regarding the cubic crystalline factor  $a$  holds satisfactorily in the case of oxides of Mg and Ca. In the case of sulfides, selenides, and tellurides, however, the prediction from this theory is not in agreement with experimental results. The disagreement is due to the covalency nature of the bonds, which is more pronounced in the heavier compounds of the two elements zinc and cadmium. Since knowledge of the sign, magnitude, and derivation of  $D$  from one-electron orbitals aids in the evaluation of  $a$ , it is necessary to find theoretical expressions for  $D$  first. Therefore, the experimental results obtained by the author and other investigators concerning hexagonal  $A_{\text{II}} B_{\text{VI}}$  compounds are given in Section II. In Section III, a theoretical discussion of the variation of the  $D$  parameter among the  $A_{\text{II}} B_{\text{VI}}$  compounds with hexagonal structure is given.





## II. RESULTS

### A. EXPERIMENTAL

Pieces of ZnSe crystals were examined in an ESR system and the microwave absorption was detected by a phase-sensitive detector. The derivative of the paramagnetic absorption with respect to the dc magnetic field,  $\frac{dx}{dH}$ , was obtained through a Varian detection and recorder system. The magnetic field associated with these resonances was measured by a Varian fluxmeter and a Beckman transfer oscillator. The resonance spectra obtained through the graphic recorder are shown in Figs. 1-4. The magnetic field was rotated in a  $(10\bar{1}0)$  plane. Figures 1a and 1b give the spectrum at  $\theta = 0$ , where the dc magnetic field is parallel to the c-axis of the crystal. Figures 2a and 2b give the spectrum at  $\theta = 25^\circ$  to the c-axis; Figs. 3a and 3b at  $\theta = 55^\circ$ ; and Figs. 4a and 4b at  $\theta = 90^\circ$ .

A comparison of these spectra indicates that the crystal is at best a twin, which is obtained by dendritic growth of ZnSe. That such a phenomenon occurs in crystals grown from melt has been observed in the growth of germanium from melt<sup>4</sup>. Due to the presence of these imperfections, the spectra are more complicated in this ZnSe than in a pure hexagonal crystal such as ZnO. Cuceaneau<sup>5</sup> reports the simultaneous presence of hexagonal and cubic structure in ZnSe. Bube<sup>6</sup>, in his detailed investigation of the optical properties of ZnSe, also reports the presence of both cubic and hexagonal structures. According to these investigations,

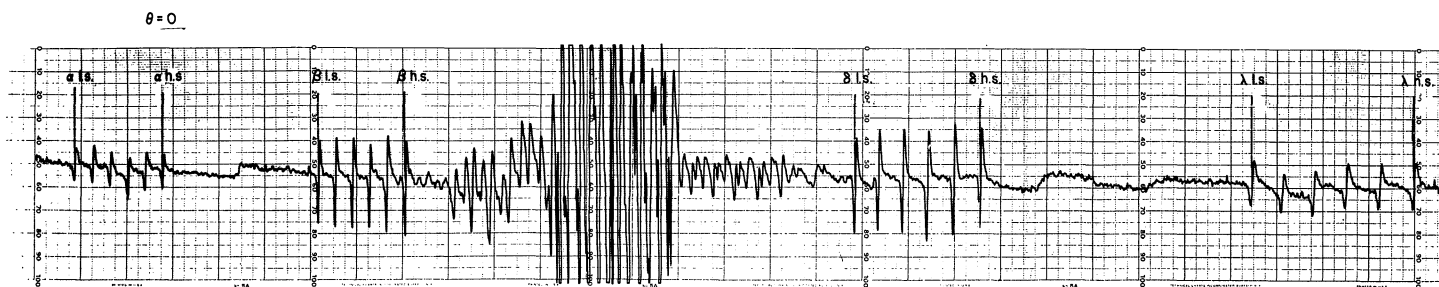


Fig. 1-a

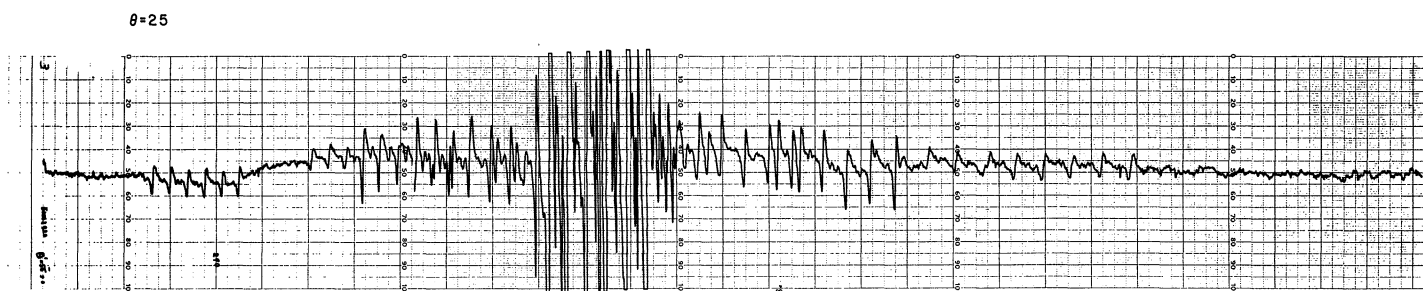


Fig. 2-a

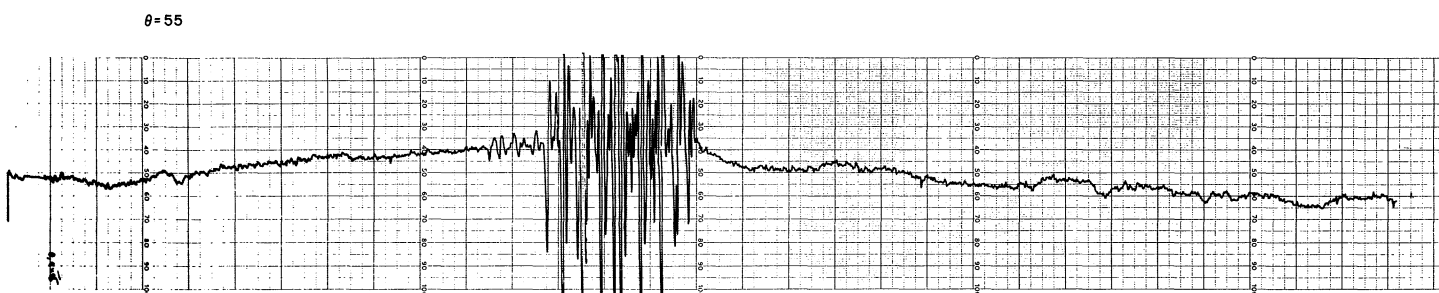


Fig. 3-a

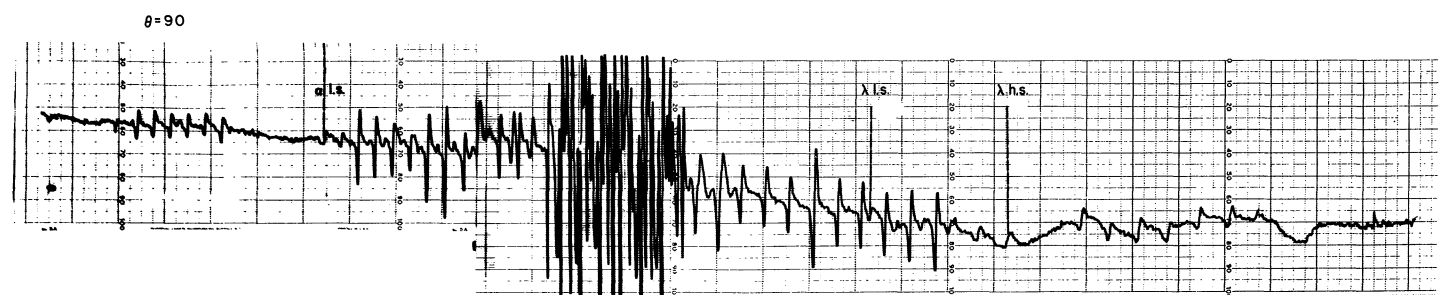


Fig. 4-a

Figs. 1a-4a. ESR Spectra of  $Mn^{++}$  in the Plane  $(10\bar{1}0)$  of ZnSe.  $\theta$  is the angle between c-axis and  $\underline{H}$ .

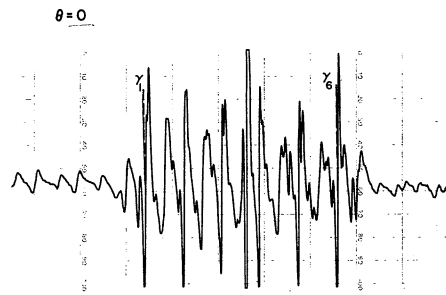


Fig. 1-b

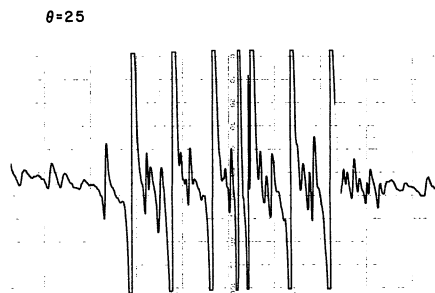


Fig. 2-b

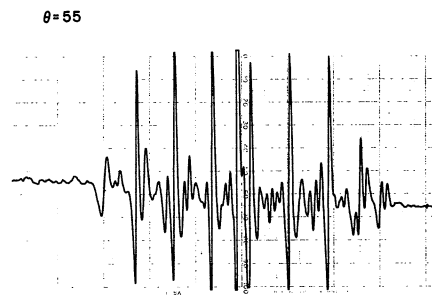


Fig. 3-b

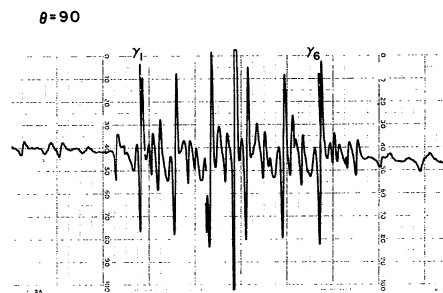


Fig. 4-b

Figs. 1b-4b. ESR Spectra of  $Mn^{++}$  in the Plane  $(10\bar{1}0)$  of ZnSe.  $\theta$  is the angle between c-axis and  $\underline{H}$ . ( $M = -1/2 \rightarrow +1/2$  transitions; signal level is reduced by a factor of 3.)

it is possible that the complexity of the central portion of the spectra shown in Figs. 1-4 is caused by the presence of microcrystallites of cubic structure. Comparing the spectra in Figs. 1a and 3a, one finds at least one spectrum behaving as though there were a hexagonal crystal, one of whose  $(10\bar{1}0)$  planes is horizontal. The measurements were carried out with respect to this set of spectra and the results for the two orientations  $\theta = 0$  and  $\theta = 90^\circ$  are given in Table I.

TABLE I  
ABSORPTION PEAK POSITIONS OF THE LINES DESIGNATED IN FIGS. 1 AND 4  
(in gauss)

$\theta$	position	$\alpha$	$\beta$	$\gamma$	$\delta$	$\lambda$	$\mu$
0	High Side	6920.70	7861.58	8745.66	9639.99	10577.08	8591.50
	Low Side	6587.51	7531.67	8420.58	9315.24	10255.68	-
	Diff = $\Delta$	333.19	329.96	325.08	324.75	321.22	-
	Average = $\sigma$	6754.10	7696.60	8583.12	9477.61	10426.29	-
90°	High Side	-	-	8745.22	-	9691.35	8590.41
	Low Side	7549.23	-	8419.61	-	9347.71	-
	$\Delta$	-	-	325.59	-	343.97	-
	$\sigma$	-	-	8582.40	-	9519.69	-

#### B. THEORETICAL

To analyze the data given in Table I the usual procedure<sup>1,2,3</sup> is to express the crystalline electric field as a function of the spin operators. This is done simply by transforming the terms of the crystalline field from the crystalline coordinate system to the magnetic coordinate system

and then substituting the spherical harmonics in the new magnetic system by Racah's  ${}^4 T_{\ell m}$  tensors. These tensors are functions of spin operators, and the coefficients of transformation from the crystalline to the magnetic coordinate system are functions of the Eulerian angles  $\alpha$ ,  $\beta$ , and  $\gamma$  through which this transformation takes place. By following this procedure one can obtain expressions which are easy to compare with experimental data.

To illustrate this procedure consider Fig. 5. The  $Mn^{++}$  ion, which is surrounded by four  $Se^{--}$  ions, is at the origin. The three  $Se^{--}$  ions, 2, 3, and 4 are equidistant from the  $Mn^{++}$  ion when the  $Se^{--}$  ion 1 is slightly further from it ( $R_1 > R_2$ ). At the  $Mn^{++}$  ion site this produces a local field of the trigonal symmetry with OA, the axis of threefold symmetry. We take as the polar axis and express the crystalline field terms in such a manner that this axis represents the z-axis of the crystalline coordinate system. The crystalline field  $V'(r, \theta, \phi)$  produced at  $Mn^{++}$  site by the neighboring ions can be expressed as a linear combination of the spherical harmonics provided  $\nabla^2 V' = 0$ :

$$V'(r, \theta, \phi) = \sum_{\ell m} A_{\ell m} Y_{\ell m}(\theta, \phi). \quad (1)$$

For the case of d-electrons of the  $Mn^{++}$  ion (the trigonal axis being the polar axis), the effective field  $V$ , when it meets the requirements of crystal symmetry,\* can be obtained from Eq. (1) by retaining only those

---

\*These requirements are that the fields by (1) real, (2) invariant under rotation  $\pm 2\pi/3$  about the c-axis, and (3) invariant under rotation  $\pi/3$  followed by reflection in a plan normal to the c-axis.

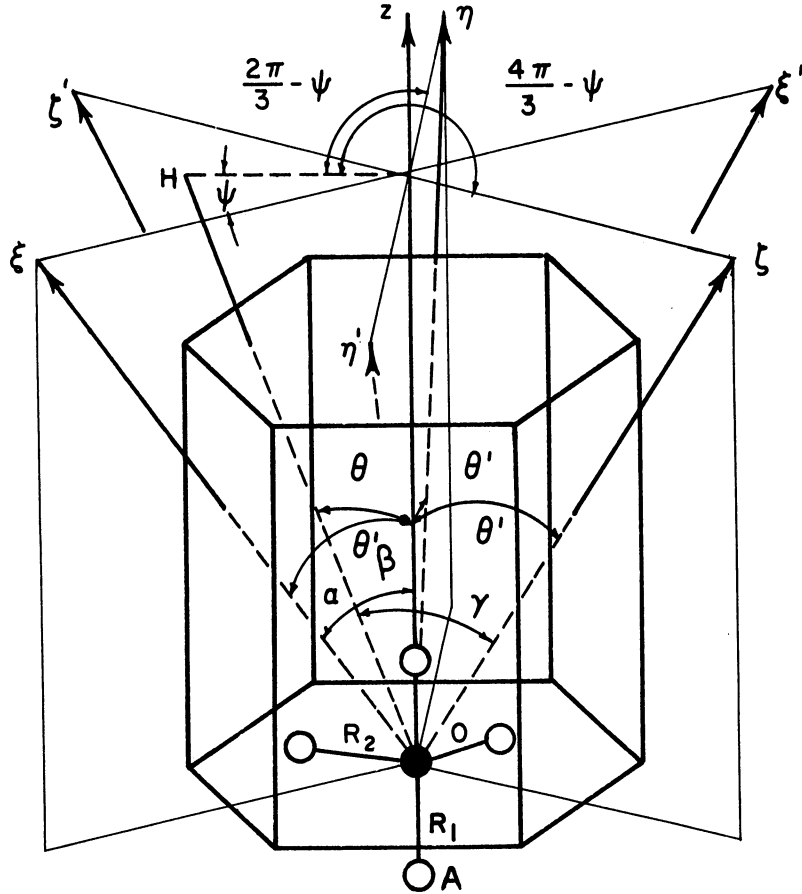


Fig. 5. Relative positions of the magnetic ( $\underline{H}$  polar axis) and crystalline coordinate systems.

terms of even  $l$  up to  $l = 4$ , with  $|m| \leq l$  and  $m$  being 0 or  $\pm 3$ . Therefore

$$V(r, \theta, \phi) = A_{00} Y_{00} + A_{20} Y_{20} + A_{40} Y_{40} + A_{43} Y_{43} + A_{4-3} Y_{4-3}, \quad (2)$$

where  $A_{lm}$ 's are independent of  $\theta$  and  $\phi$  and are numerical constants multiplied by  $r^l$ . Since the term  $A_{00} Y_{00}$  shifts all of the spin levels by the same amount, it does not produce any change in the relative energies of the levels. The coefficients  $A_{4\pm 3}$  are related to each other. To find this relation, use will be made of symmetry operations on the  $xyz$  coordin-

ate system. Before doing so we write Eq. (2) as a sum of two axial and cubic terms  $V_a$  and  $V_c$ :

$$V(r, \theta, \phi) \implies V(xyz) = V_a(xyz) + V_c(xyz), \quad (3)$$

$$V_a(xyz) = A_{00} Y_{00} + A_{20} Y_{20} + A'_{40} Y_{40}, \quad (4)$$

$$V_c(xyz) = A''_{40} Y_{40} + A_{43} Y_{43} + A_{4-3} Y_{4-3}, \quad (5)$$

where<sup>7</sup>

$$Y_{40}(xyz) = \sqrt{\frac{9}{4\pi}} (35Z^4 - 30Z^2 r^2 + 3r^4) / 8r^4, \quad (6)$$

$$Y_{4\pm 3}(xyz) = \sqrt{\frac{9}{4\pi}} \frac{35}{16} z (x \pm iy)^3 / r^4. \quad (7)$$

Substituting for  $Y_{40}$  and  $Y_{4\pm 3}$  in Eq. (5) and operating with  $C_2$  (face diagonal =  $yy'$ ), we find:

$$C_2 V_c(xyz) = V_c(-x, y, -z). \quad (8)$$

Since  $C_2$  is a symmetry axis of the cube (Fig. 6),  $V_c(x, y, z) = V_c(-x, y, -z)$ , resulting in

$$A_{43} = -A_{4-3} \quad (9)$$

or

$$V_c(xyz) = A''_{40} Y_{40} + A_{43} (Y_{43} - Y_{4-3}). \quad (10)$$

There is also a numerical relation between  $A''_{40}$  and  $A_{43}$ , which can be



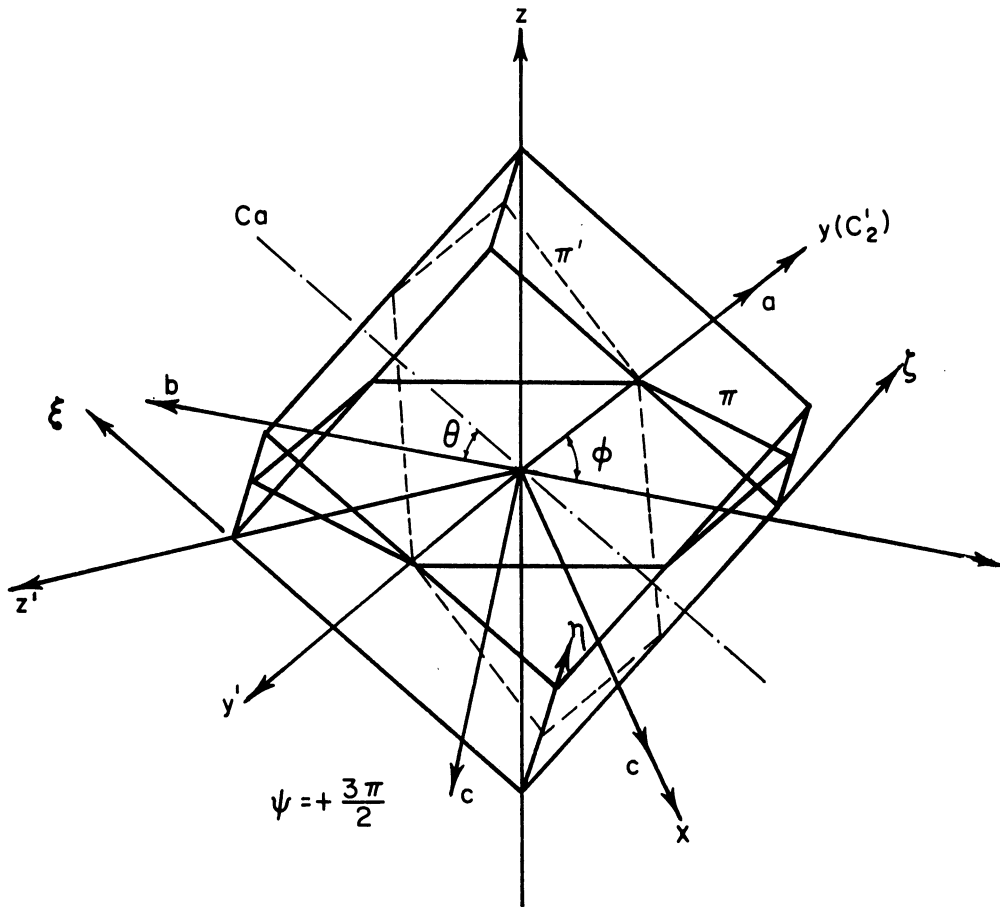


Fig. 6. Change of the axis of quantization ( $z$ -axis) from  $[100]$  to  $[111]$  direction and the result of  $C_2$  operation on  $xyz$ .

obtained by operating on  $V_c(xyz)$  with  $C_2$  axis of symmetry (Fig. 6). This operation brings the  $xyz$  system into the  $x'y'z'$  system. A close inspection of Fig. 6 reveals that this operation is equivalent to the initially orthogonal rotations  $\phi = \pi/2$ ,  $\theta = \cos^{-1}(-1/3)$ , and  $\psi = 3\pi/2$ , around the  $z$ , the  $a$ , and the  $z'$  axes respectively. Therefore

$$\begin{aligned}
\begin{pmatrix} x' \\ y' \\ z' \end{pmatrix} &= \begin{pmatrix} \cos\psi & \sin\psi & 0 \\ -\sin\psi & \cos\psi & 0 \\ 0 & 0 & 1 \end{pmatrix} \begin{pmatrix} 1 & 0 & 0 \\ 0 & \cos\theta & \sin\theta \\ 0 & -\sin\theta & \cos\theta \end{pmatrix} \begin{pmatrix} \cos\psi & \sin\psi & 0 \\ -\sin\psi & \cos\psi & 0 \\ 0 & 0 & 1 \end{pmatrix} \begin{pmatrix} x \\ y \\ z \end{pmatrix} \\
&= \begin{pmatrix} 0 & -1 & 0 \\ 1 & 0 & 0 \\ 0 & 0 & 1 \end{pmatrix} \begin{pmatrix} 1 & 0 & 0 \\ 0 & -1/3 & 2\sqrt{2/3} \\ 0 & -2\sqrt{2/3} & -1/3 \end{pmatrix} \begin{pmatrix} 0 & 1 & 0 \\ -1 & 0 & 0 \\ 0 & 0 & 1 \end{pmatrix} \begin{pmatrix} x \\ y \\ z \end{pmatrix} \\
&= \begin{pmatrix} -1/3 & 0 & 2\sqrt{2/3} \\ 0 & -1 & 0 \\ 2\sqrt{2/3} & 0 & 1/3 \end{pmatrix} \begin{pmatrix} x \\ y \\ z \end{pmatrix}.
\end{aligned} \tag{11}$$

Since  $C_2$  is a symmetry axis, as in the case of  $C_2$  we have  $C_2V_c = V_c$ . Substituting for  $Y_{lm}$ 's in  $V_c(x,y,z)$  from Eqs. (6-7) and employing the transformation represented by Eq. (11), one obtains:

$$\begin{aligned}
&r^{-4}A_{40}'' \sqrt{\frac{9}{4\pi}} \left[ \frac{1}{8} \left\{ 35z^4 - 30z^2r^2 + 3r^4 - (A_{43}/A_{40}'') \sqrt{\frac{35}{16}} \{ z(x+iy)^3 + z(x-iy)^3 \} \right\} \right] \\
&= r^{-4}A_{40}'' \sqrt{\frac{9}{4\pi}} \left[ \frac{1}{8} \left\{ 35 \left( 2\sqrt{\frac{x}{3}} - \frac{2}{3} \right)^4 - 30 \left( \frac{2\sqrt{2x}}{3} - \frac{2}{3} \right)^2 r^2 + 3r^4 \right. \right. \\
&\quad \left. \left. - (A_{43}/A_{40}'') \sqrt{\frac{35}{16}} \left\{ \left( \frac{2\sqrt{2x}}{3} - \frac{2}{3} \right) \left[ \left( \frac{x}{3} + \frac{2\sqrt{2x}}{3} - iy \right)^3 + \left( \frac{x}{3} + \frac{2\sqrt{2x}}{3} + iy \right)^3 \right] \right\} \right\} \right].
\end{aligned} \tag{12}$$

Equation (12) holds if the coefficients of each power of  $x$ ,  $y$ , or  $z$  are the same on both sides. We will take the coefficients of  $z^4$ :

$$\begin{aligned}
\frac{1}{8}(35-30+3) &= \frac{1}{8} \left( \frac{35}{81} - \frac{30}{9} + 3 \right) - (A_{43}/A_{40}'') \left\{ -\frac{2}{3} \left( \frac{2\sqrt{2}}{3} \right)^3 \right\} A_{43}/A_{40}'' \tag{13} \\
&= \sqrt{10/7}.
\end{aligned}$$

Thus, the cubic part of the crystalline field  $V_c(x,y,z)$  is

$$V_{c\pm} = A_{40}'' [Y_{40} \pm \sqrt{10/7} (Y_{43} - Y_{4-3})]. \tag{14}$$

The  $V_{c-}$  belongs to the field produced on those  $Mn^{++}$  ions which are surrounded by tetrahedrons of ligands represented by  $\xi', \eta', \zeta'$  (Fig. 5).

We must now find the matrix elements of these  $V_a$  and  $V_{c\pm}$  between the magnetic states of the  $Mn^{++}$  ion. This can be done by transforming  $V_a$  and  $V_{c\pm}$  into a magnetic coordinate system where  $\underline{H}$ , the dc magnetic field, is considered the z-axis. The transformation of  $V_a$  and  $V_{c\pm}$  involves the transformation of the spherical harmonics  $Y_{lm}$ . These spherical harmonics transform like the monomials  $\xi^{\ell+m} \eta^{\ell-m} / [(\ell+m)!(\ell-m)!]$  where  $\xi$  and  $\eta$ , under a rotation of the coordinate system through the Eulerian angles  $\alpha$ ,  $\beta$ , and  $\gamma$ , transform into  $\xi'$  and  $\eta'$  as follows\*:

$$\begin{pmatrix} \xi' \\ \eta' \end{pmatrix} = \begin{pmatrix} a & b \\ -b^* & a^* \end{pmatrix} \begin{pmatrix} \xi \\ \eta \end{pmatrix} \quad (15)$$

where

$$a = e^{-i\alpha/2} \cos \beta e^{-\gamma/2}, \quad b = -e^{-i\alpha/2} \sin \frac{\beta}{2} e^{i\gamma/2}.$$

The coefficients of transformation of  $Y_{lm}$  are<sup>6</sup>

$$D^{(\ell)}(\{\alpha, \beta, \gamma\})_{m'm} = \sum_{\lambda} (-1)^{\lambda} \frac{\sqrt{(\ell-m)!(\ell+m)!(\ell-m')!(\ell+m')!}}{(\ell-m'-\lambda)!(\ell+m-\lambda)!\lambda!(\lambda+m'-m)!} \\ (x) e^{im'\alpha} \cos^{2\ell+m-m'-2\lambda} \frac{\beta}{2} \sin^{-m+m'+2\lambda} \quad (16) \\ (x) \frac{\beta}{2} e^{imy}.$$

Considering the axial nature of the spectra (Figs. 1a-4a), we obtain  $D_{m'0}^{(2)}$  for  $m' = -2, -1, 0, 1, \text{ and } 2$  for  $Y_{2m}$  terms, whereas for  $Y_{4m}$  terms we find only the terms corresponding to  $D_{00}^{(4)}$  and  $D_{03}^{(4)}$ . It is necessary to note

---

\*Do not confuse  $\xi$ ,  $\eta$ ,  $\xi'$  and  $\eta'$  with the  $\xi\eta\zeta$  and  $\xi'\eta'\zeta'$  above.

that the angle  $\gamma$  in Wigner's notation is similar to  $\phi$  of the Goldstein  $\pm \pi/2$ . For the case where the magnetic field is in one of the planes parallel to the c-axis we can take  $\alpha = 0$ . Therefore we find only  $D_{m'm}^{(\ell)}(0, \beta, \gamma)$ , as follows:

$$D_{m'o}^{(2)}(0, \beta, \gamma) = \sum_{\lambda} (-1)^{\lambda} \frac{2 \sqrt{2-m'}! (2+m')!}{(2-m'-\lambda)! (2-\lambda)! \lambda! (2+m')!} \cos^{4-m'-2\lambda} \left( \frac{\beta}{2} \right) \quad (17)$$

$$(x) \sin^{m'+2\lambda} \left( \frac{\beta}{2} \right).$$

Therefore

$$D_{oo}^{(2)}(0, \beta, \gamma) = 4 \left[ \frac{1}{4} \cos^4 \left( \frac{\beta}{2} \right) - \cos^2 \left( \frac{\beta}{2} \right) \sin^2 \left( \frac{\beta}{2} \right) + \frac{1}{4} \sin^4 \left( \frac{\beta}{2} \right) \right]$$

$$= \left[ \cos^2 \left( \frac{\beta}{2} \right) - \sin^2 \left( \frac{\beta}{2} \right) \right]^2 - \frac{1}{2} \left[ 2 \sin \left( \frac{\beta}{2} \right) \cos \left( \frac{\beta}{2} \right) \right]^2 \quad (18)$$

$$= \frac{1}{2} (3 \cos^2 \beta - 1),$$

$$D_{10}^{(2)}(0, \beta, \gamma) = \sum_{\lambda} (-1)^{\lambda} \frac{\sqrt{6}}{(1-\lambda)! (2-\lambda)! \lambda! (\lambda+1)!} \cos^{3-2\lambda} \frac{\beta}{2} \sin^{1+2\lambda} \frac{\beta}{2}$$

$$= \frac{\sqrt{6}}{2} \left( \cos \frac{\beta}{2} \sin \frac{\beta}{2} - \cos \frac{\beta}{2} \sin \frac{\beta}{2} \right) \quad (19)$$

$$= \frac{\sqrt{6}}{4} \sin \beta \cos \beta,$$

and

$$D_{20}^{(2)}(0, \beta, \gamma) = \sum_{\lambda} (-1)^{\lambda} \frac{4}{(-\lambda)! (2-\lambda)! \lambda! (\lambda+2)!} \cos^{2-2\lambda} \left( \frac{\beta}{2} \right) \sin^{2+2\lambda} \left( \frac{\beta}{2} \right) \quad (20)$$

$$= \cos^2 \frac{\beta}{2} \sin^2 \frac{\beta}{2} = \frac{1}{4} \sin^2 \beta.$$

Since  $D_{m'm}^{(\ell)}(0, \beta, \gamma)$  coefficients are real, it is obvious that

$$D_{-m'm}^{(\ell)}(0, \beta, \gamma) = (-1)^{m'} D_{m'm}^{(\ell)}(0, \beta, \gamma), \quad (21)$$

giving

$$D_{-10}^{(2)}(0, \beta, \gamma) = -\frac{\sqrt{6}}{4} \sin \beta \cos \beta \quad (22)$$

and

$$D_{-20}^{(2)}(0, \beta, \gamma) = \frac{1}{4} \sin^2 \beta. \quad (23)$$

For transforming the remaining terms, it is necessary to find  $D_{00}^{(4)}$  and  $D_{03}^{(4)}$ :

$$\begin{aligned} D_{00}^{(4)}(0, \beta, \gamma) &= \sum_{\lambda} (-1)^{\lambda} \frac{(4!)^2}{[(4-\lambda)!]^2 (\lambda!)^2} \cos^{8-2\lambda} \frac{\beta}{2} \sin^{2\lambda} \frac{\beta}{2} \\ &= \cos^8 \frac{\beta}{2} - \frac{(4!)^2}{(3!)^2} \cos^6 \frac{\beta}{2} \sin^2 \frac{\beta}{2} + \frac{(4!)^2}{(2!)^4} \cos^4 \frac{\beta}{2} \sin^4 \frac{\beta}{2} \\ &\quad - \frac{(4!)^2}{(3!)^2} \cos^2 \frac{\beta}{2} \sin^6 \frac{\beta}{2} + \sin^8 \frac{\beta}{2} \\ &= \left( \cos^2 \frac{\beta}{2} - \sin^2 \frac{\beta}{2} \right)^2 - 3 \cos^2 \beta (1 - \cos^2 \beta) \\ &\quad + \frac{3}{8} (1 - 2 \cos^2 \beta + \cos^4 \beta) = \frac{1}{8} [8 \cos^4 \beta + 24 \cos^4 \beta - 24 \cos^2 \beta \\ &\quad + 3 - 6 \cos^2 \beta + 3 \cos^4 \beta] = \frac{1}{8} [35 \cos^4 \beta - 30 \cos^2 \beta + 3], \end{aligned} \quad (24)$$

and

$$\begin{aligned} D_{03}^{(4)} &= \sum_{\lambda} (-1)^{\lambda} \frac{4! \sqrt{7!}}{(4-\lambda)! (7-\lambda)! \lambda! (\lambda-3)!} \cos^{11-2\lambda} \left( \frac{\beta}{2} \right) \sin^{-3+2\lambda} \left( \frac{\beta}{2} \right) e^{i3\gamma} \\ &= -4 \sqrt{7!} \left[ \frac{1}{4! 3!} \cos^5 \frac{\beta}{2} \sin^3 \frac{\beta}{2} e^{i3\gamma} - \frac{1}{4! 3!} \cos^3 \frac{\beta}{2} \sin^5 \frac{\beta}{2} e^{i3\gamma} \right] \\ &= -\frac{\sqrt{7!}}{8 \cdot 3!} e^{i3\gamma} \sin^3 \beta \cos \beta. \end{aligned} \quad (25)$$

It is evident that

$$D_{0-3}^{(4)} = + \frac{\sqrt{7!}}{8.3!} e^{-3i\gamma} \sin^3 \beta \cos \beta. \quad (26)$$

Considering the Eqs. (3-5) and substituting for  $Y_{20}$ ,  $Y_{40}$ , and  $Y_{4\pm 3}$ , one finds for the transformed potential in the magnetic coordinate system

$V'(\theta', \phi', \beta, \gamma, r)$ :

$$\begin{aligned} V'(\theta', \phi', \beta, \gamma, r) &= A_{00} Y_{00} + A_{20} \sum_{m'=-2}^2 D_{m'0}^{(2)}(0, \beta, \gamma) Y_{2m}(\theta', \phi') \\ &+ A_{40} D_{00}^{(4)}(0, \beta, \gamma) Y_{40}(\theta', \phi') + A_{40}'' [D_{00}^{(4)}(0, \beta, \gamma) \\ &\pm \sqrt{\frac{10}{7}} D_{03}^{(4)}(0, \beta, \gamma) (Y_{43}(\theta', \phi') - Y_{4-3}(\theta', \phi'))]. \end{aligned} \quad (27)$$

The electric field represented by Eq. (27) does not predict any splitting of the magnetic levels of  $Mn^{++}$  ions; but a splitting of the levels does exist (see Fig. 1a-4a), and Eq. (27) must be modified to include the spin operators. This has been done by Bleaney and Stevens<sup>9</sup> by a method similar to the one they used for substitution of  $Y_{\ell \pm m}(\theta', \phi')$  with  $L_{\pm}$  operators. An alternative procedure is suggested by Kikuchi and Matarrese<sup>10</sup>: instead of writing the  $Y_{\ell m}(\theta', \phi')$  as a function of  $x$ ,  $y$ , and  $z$  [see Eqs. (6-7)] and then substituting  $x$ ,  $y$ , and  $z$  with appropriate linear combinations of  $s_x$ ,  $s_y$ , and  $s_z$  as shown elsewhere<sup>2</sup>, one can substitute those  $Y_{\ell m}$  functions with Racah's<sup>11</sup>  $T_{kq}$  tensors. These tensors are generated by the process

$$T_{kq-1} = [k *^2 - q(q-1)]^{-1/2} [S-, T_{kq}]. \quad (28)$$

To obtain all terms of Eq. (27) as functions of the spin operators, we have to define  $T_{22}$  and  $T_{44}$ . According to Kikuchi and Matarrese they can be taken as:

$$T_{2\pm 2} = 6^{-1/2} S_{\pm}^2, \quad T_{4\pm 4} = (16)^{-1} \sqrt{70} S_{\pm}^4. \quad (29)$$

Substituting from Eqs. (28-29) for the  $Y_{\ell m}$ 's of Eq. (27), and substituting from Eqs. (18-26) for the  $D_{m'm}^{(\ell)}(\alpha, \beta, \gamma)$  of Eq. (16), one obtains

$$\begin{aligned} V'(r, \theta', \phi', \beta, \gamma) - A_{00} Y_{00} &= \pi A_{20} \left[ \frac{1}{2} (3 \cos^2 \beta - 1) T_{20} + \pi_1 \sin \beta \cos \beta \right. \\ &\quad (x) (T_{21} - T_{2-1} + \pi_2 \sin^2 \beta (T_{22} + T_{2-2})) + \frac{\pi'}{8} A_{40} \\ &\quad (x) (35 \cos^4 \theta - 30 \cos^2 \theta + 3) T_{40} + \frac{\pi''}{8} A_{40}'' \\ &\quad (x) \left[ (35 \cos^4 \beta - 30 \cos^2 \beta + 3) T_{40} \pm 8 \sqrt{\frac{10}{7}} \pi_3 \sin^3 \beta \right. \\ &\quad \left. (x) \cos \beta (e^{3i\gamma} T_{43} - e^{-3i\gamma} T_{4-3}), \right] \quad (30) \end{aligned}$$

where the  $\pi$  parameters are numerical constants arising from the substitution of  $T_{\ell m}$ 's for  $Y_{\ell m}$ 's. The energy associated with each magnetic level  $M, m$  of the  $Mn^{++}$  ion to the second-order perturbation can be found from the Hamiltonian

$$\mathcal{H} = g\beta \underline{S}' \cdot \underline{H} + A \underline{I} \cdot \underline{S}' + V' - A_{00} Y_{00} - g_N \beta_N \underline{H} \cdot \underline{I} \quad (31)$$

and is

$$\begin{aligned} E_{Mm}(\beta, \gamma) &= E_{Mm}^f + E_{Mm}^h \\ &= E_{Mm}^{f(0)} + E_{Mm}^{f(1)} + E_{Mm}^{f(2)} \\ &\quad + E_{Mm}^{h(1)} + E_{Mm}^{h(2)}, \quad (32) \end{aligned}$$

where  $f$  and  $h$  denote the fine and hyperfine structure and  $M$  and  $m$  the electron and nuclear spin quantum numbers respectively. For transitions due to  $\Delta M = \pm 1$  and  $\Delta m = 0$  corresponding to  $[E_{Mm}(\beta, \gamma) - E_{M-1, m}(\beta, \gamma)]/g\beta$ , we

will find\*:

$$\begin{aligned} H \left[ M = \pm \frac{5}{2} \leftrightarrow \pm \frac{3}{2}, m, \beta, \gamma \right] &= H_0 \pm \left\{ 4DF_1 + 2pa + \frac{1}{6}F_a \right\} - 32 \frac{D^2}{H} F_2 \\ &+ \frac{D^2}{H} F_3 - Am - \frac{A^2}{2H_0} \left[ \frac{35}{4} - m^2 \pm 4m \right] + \epsilon_1; \end{aligned} \quad (33)$$

$$\begin{aligned} H \left[ M = \pm \frac{5}{2} \leftrightarrow \pm \frac{3}{2}, m, \beta, \gamma + \pi \right] &= H_0 \mp \left\{ 4DF_1 + 2p'a + \frac{1}{6}F_a \right\} \\ &- 32 \frac{D^2}{H_0} F_2 + \frac{D^2}{H_0} F_3 - Am - \frac{A^2}{2H_0} \left[ \frac{35}{4} - m^2 \pm 4m \right] + \epsilon_1, \end{aligned}$$

$$\begin{aligned} H \left[ M = \pm \frac{3}{2} \leftrightarrow \pm \frac{1}{2}, m, \beta, \gamma \right] &= H_0 \mp \left\{ 2DF_1 - \frac{5}{2}pa - \frac{5}{24}F_a \right\} + \frac{4D^2}{H_0} F_2 \\ &- \frac{5}{4} \frac{D^2}{H_0} F_3 - Am - \frac{A^2}{2H_0} \left[ \frac{35}{4} - m^2 \pm 2m \right] + \epsilon_2; \end{aligned} \quad (34)$$

$$\begin{aligned} H \left[ M = \pm \frac{3}{2} \leftrightarrow \pm \frac{1}{2}, m, \beta, \gamma + \pi \right] &= H_0 \mp \left\{ 2DF_1 - \frac{5}{2}p'a - \frac{5}{24}F_a \right\} \\ &+ \frac{4D^2}{H_0} F_2 - \frac{5}{4} \frac{D^2}{H_0} F_3 - Am - \frac{A^2}{2H_0} \left[ \frac{35}{4} - m^2 \pm 2m \right] + \epsilon_2; \end{aligned} \quad (35)$$

and

$$H \left[ M = \pm \frac{1}{2} \leftrightarrow -\frac{1}{2}, m, \beta, \gamma \right] = H_0 + \frac{16D^2}{H_0} F_2 - \frac{2D^2}{H_0} F_3 + \epsilon_3, \quad (36)$$

where  $D = \pi A_{20}$  is the so-called axial field splitting of second degree ( $l = 2$ );  $F$  is the axial field splitting parameter of fourth degree ( $l = 4$ ) related to  $A_{40}$  [Eq. (30)];  $a$  is the cubic field parameter associated with  $A_{40}$ ;  $F_1$  corresponds to the first-order perturbation and  $F_2$  and  $F_3$  to the

---

\*Do not confuse  $\beta, \gamma$  with  $\beta$  in  $g\beta$ , which is Bohr magneton.



second-order perturbation; and  $p$ ,  $p'$ , and  $g$  are related to  $\pi'A'_{H_0}$  and  $\pi''A''_{H_0}$ . These parameters can be obtained from Eq. (30) as follows:

$$F_1 = \frac{1}{2}(3 \cos^2\beta - 1), \quad (37)$$

$$F_2 = \sin^2\beta \cos^2\beta, \quad (38)$$

$$F_3 = \sin^4\beta, \quad (39)$$

$$g = 35 \cos^4\beta - 30 \cos^2\beta + 3, \quad (40)$$

$$p, p' = -\frac{g}{12} \pm \sin^3\beta \cos 3\gamma \quad (41)$$

The coefficients  $\epsilon_1$ ,  $\epsilon_2$ , and  $\epsilon_3$  are derived elsewhere<sup>12</sup> and have the values

$$\epsilon_1 = a^2 \left\{ \frac{5}{3} \phi (1 - 7\phi) \right\} / H_0, \quad (42)$$

$$\epsilon_2 = -a^2 \{ 5(3 + 178\phi - 625\phi^2) / 48 \} / H_0, \quad (43)$$

$$\epsilon_3 = a^2 \{ 10\phi(7 - 25\phi) / 3 \} / H_0, \quad (44)$$

where

$$\phi = l^2 m^2 + m^2 n^2 + n^2 l^2, \quad (45)$$

$l$ ,  $m$ ,  $n$  being the direction cosines of  $H$  referred to  $\xi\eta\zeta$  axes of the cubic field. [See Fig. 5 and recall that  $\alpha, \beta, \gamma$  here are not necessarily the same as those in  $D_{m'm}^{(l)}(\alpha, \beta, \gamma)$ ]. Comparison of Figs. 1-4 reveals that the magnetic field lies in the  $(10\bar{1}0)$  plane of the hexagon; thus  $\gamma = \pi/6$  and  $\gamma' = 7\pi/6$  yields  $p = p' = -g/12$ . For this special case one has (putting

$$\beta = \theta)$$

$$\begin{aligned} H \left[ M = \pm \frac{5}{2} \leftrightarrow \pm \frac{3}{2}, m, \theta \right] &= H_0 \mp \left\{ 2D(3^2 \cos^2 \theta - 1) - \frac{a-F}{6} \right. \\ &\quad \left. (x) (35 \cos^4 \theta - 30 \cos^2 \theta + 3) \right\} - 32 \frac{D^2}{H_0} \cos^2 \theta \sin^2 \theta \\ &\quad + \frac{D^2}{H_0} \sin^4 \theta - Am - \frac{A^2}{2H_0} \left( \frac{35}{4} - m^2 \pm 4m \right) + \epsilon_1, \end{aligned} \quad (46)$$

$$\begin{aligned} H \left[ M = \pm \frac{3}{2} \leftrightarrow \pm \frac{1}{2}, m, \beta = \theta, r = \frac{\pi}{6} \right] &= H_0 \mp \left\{ D(3 \cos^2 \theta - 1) + \frac{5}{4}(a-F) \right. \\ &\quad \left. (x) \frac{35 \cos^4 \theta - 30 \cos^2 \theta + 3}{6} \right\} + 4 \frac{D^2}{H_0} \cos^2 \theta \sin^2 \theta - \frac{5}{4} \frac{D^2}{H_0} \sin^4 \theta - mA \\ &\quad - \frac{A^2}{2H_0} \left( \frac{35}{4} - m^2 \pm 2m \right) + \epsilon_2, \end{aligned} \quad (47)$$

$$\begin{aligned} H \left[ M = \frac{1}{2} \rightarrow -\frac{1}{2}, m, \beta = \theta, r = \frac{\pi}{6} \right] &= H_0 + \frac{16D^2}{H_0} \sin^2 \theta \cos^2 \theta - \frac{2D^2}{H_0} \sin^4 \theta \\ &\quad - mA - \frac{A^2}{2H_0} \left( \frac{35}{4} - m^2 \right) + \epsilon_3. \end{aligned} \quad (48)$$

For  $\theta = 0$ ,

$$\begin{aligned} H \left[ M = \frac{3}{2} \rightarrow \frac{5}{2}, \theta = 0, m \right] - H_0 &= -4D + \frac{4}{3}(a-F) \\ &\quad - Am - \frac{A^2}{2H_0} \left( \frac{35}{4} - m^2 + 4m \right) + \epsilon_1, \end{aligned} \quad (49)$$

$$\begin{aligned} H \left[ M = \frac{1}{2} \rightarrow \frac{3}{2}, \theta = 0, m \right] - H_0 &= -2D - \frac{5}{3}(a-F) \\ &\quad - Am - \frac{A^2}{2H_0} \left( \frac{35}{4} - m^2 + 2m \right) + \epsilon_2, \end{aligned} \quad (50)$$

$$H \left[ M = -\frac{1}{2} \rightarrow \frac{1}{2}, \theta = 0, m \right] - H_0 = -Am - \frac{A^2}{2H_0} \left( \frac{35}{4} - m^2 \right) + \epsilon_3, \quad (51)$$

$$\begin{aligned}
H \left[ M = -\frac{3}{2} \rightarrow -\frac{1}{2}, \theta = 0, m \right] - H_0 &= 2D + \frac{5}{3}(a-F) \\
- Am - \frac{A^2}{2H_0} \left( \frac{35}{4} - m^2 - 2m \right) + \epsilon_2, & \quad (52)
\end{aligned}$$

and

$$\begin{aligned}
H \left[ M = -\frac{5}{2} \rightarrow -\frac{3}{2}, \theta = 0, m \right] - H_0 &= 4D - \frac{4}{3}(a-F) \\
- Am - \frac{A^2}{2H_0} \left( \frac{35}{4} - m^2 - 4m \right) + \epsilon_1. & \quad (53)
\end{aligned}$$

In all the  $A_{II} B_{VI}$  compounds of sphalerite and Wurtzite structures studied so far, A has been found to be negative. Therefore the low side and high side fine-structure components such as  $\alpha_{LS} \dots \alpha_{HS} \dots$ ,  $\delta_{LS} \dots$  and  $\delta_{HS} \dots$  (see Figs. 1a-4a) are related to  $m = -5/2$  and  $m = +5/2$  respectively. It is also wellknown that the relative intensities of the resonances corresponding to  $M = \pm 5/2 \leftrightarrow \pm 3/2$ ,  $\pm 3/2 \leftrightarrow \pm 1/2$  and  $-1/2 \rightarrow 1/2$  transitions vary as 5:8:9. Thus the transitions  $\alpha_1 \dots \alpha_6$  and  $\delta_1 \dots \delta_6$  (see Figs. 1a-4a) represent the  $M = \pm 5/2 \leftrightarrow \pm 3/2$  transitions. Considering Eqs. (49) and (51), one has

$$\begin{aligned}
\Delta \left( \pm \frac{5}{2}, \pm \frac{3}{2} \right) &= H \left( \pm \frac{5}{2} \leftrightarrow \pm \frac{3}{2}, m = +\frac{5}{2} \right) - H \left( \pm \frac{5}{2} \leftrightarrow \pm \frac{3}{2}, m = -\frac{5}{2} \right) \\
&= -5A \mp 10A^2/H_0. \quad (54)
\end{aligned}$$

Equation (54) indicates that  $\Delta$  for  $-5/2 \rightarrow -3/2$  transitions should be greater than  $\Delta$  for  $3/2 \rightarrow 5/2$  transitions. Comparing the data in Table I and Eq. (54), we find that  $\alpha$ -,  $\beta$ -,  $\gamma$ -,  $\delta$ -, and  $\lambda$ - absorptions in Fig. 1a correspond to  $M = -5/2 \rightarrow -3/2$ ,  $-3/2 \rightarrow -1/2$ ,  $-1/2 \rightarrow 1/2$ ,  $1/2 \rightarrow 3/2$ , and

3/2 → 5/2 transition respectively, and that the individual lines such as  $\alpha_1 \dots \alpha_6$  in each group correspond to nuclear magnetic quantum numbers ranging from  $m = -5/2$  for  $\alpha_1$  to  $m = +5/2$  for  $\alpha_6$ .

### C. DETERMINATION OF $g$ , $A$ , $D$ , $a$ , and $F$

To compute  $g$  [Eq. (30)], a strong set of six lines corresponding to  $\gamma$  transitions (Fig. 1a) has been considered. This set is believed to belong to the cubic crystallites inside the crystal. The  $g$  factors at  $\theta = 0$  and  $\theta = 90^\circ$  are obtained through hydrazyl with the magnetic probe being located close to the bottom of k-band cylindrical cavity:

$$\begin{aligned} g_{11}(\theta = 0) &= 2.0056 \\ g_{\perp}(\theta = 90^\circ) &= 2.0055 \end{aligned} \tag{55}$$

A comparison with  $\alpha$ ,  $\beta$ ,  $\delta$ , and  $\lambda$  transitions reveals that the  $g$  corresponding to the hexagonal components is slightly smaller, and that at  $\theta = 0$  we have

$$g_{11}^h(\theta = 0) \cong 2.0050 \tag{56}$$

The computation of  $A$  has been carried out through the relation

$$|A| \cong \frac{1}{5} (\gamma_6 - \gamma_1)$$

with the following results:

$$\begin{aligned} A^c &= -65.09 \text{ gauss or } -60.86 \times 10^{-4} \text{ cm}^{-1}, \\ A_{11}^c &= -65.02 \text{ gauss or } -60.78 \times 10^{-4} \text{ cm}^{-1}, \end{aligned} \tag{57}$$

and

$$A_{11}^h = - 65.44 \text{ gauss or } - 61.18 \times 10^{-4} \text{ cm}^{-1}.$$

Considering Eqs. (49-53) and Table I, one finds:

$$\begin{cases} - 8D + \frac{8}{3}(a-F) = 3672.19 \text{ gauss} \\ - 4D - \frac{10}{3}(a-F) = 1781.01 \text{ gauss,} \end{cases} \quad (58)$$

giving

$$D = - 455.03 \text{ gauss or } - 425.1 \times 10^{-4} \text{ cm}^{-1}. \quad (59)$$

Equations (58) give:

$$a-F = 11.8 \text{ gauss or } 11.05 \times 10^{-4} \text{ cm}^{-1}.$$

It is found<sup>13</sup> that

$$a = 17.66 \times 10^{-4} \text{ cm}^{-1}; \quad (60)$$

therefore

$$F = + 6.61 \times 10^{-4} \text{ cm}^{-1}. \quad (61)$$

### III. DISCUSSION

In Table II the parameters  $g$ ,  $A$ ,  $D$ ,  $a$ , and  $F$  corresponding to the hexagonal  $A_{II} B_{VI}$  compounds ZnO, ZnS, ZnSe, CdS, and CdSe are given.

TABLE II  
Mn<sup>++</sup> ESR PARAMETERS IN HEXAGONAL  $A_{II} B_{VI}$  COMPOUNDS

Crystal	$g$	$A \times 10^4 \text{ cm}^{-1}$	$D \times 10^4 \text{ cm}^{-1}$	$a \times 10^4 \text{ cm}^{-1}$	$F \times 10^4 \text{ cm}^{-1}$	T(OK)	Ref.
ZnO	2.0016±6	-76.0±.4	-216.9±2.2	+6±1.5*	-	77	a
ZnS	2.0016±1	-65±1	-105±2		-7.6±1**	-	b
ZnSe	2.0050±5	-61.2±5	-425.1±1	+17.66	+6.61	300	c
CdS	2.0029±6	-65.3±4	+8.2±2.2	+4.2±1.5*		300	a
CdSe	2.0042±10	-62.7±.5	+15.2±.5	+14.3±1	-2±1	77°	d

\*In ZnO and CdS these  $a$  factors should be considered  $a-F$

\*\* $F$  here is actually  $a-F$

- References:
- P. Dorain, Phys. Rev. 112, 1058 (1958).
  - Keiler et al., Phys. Rev. 110, 850 (1958).
  - This paper.
  - Reuben Title, Phys. Rev. 130, 17 (1963).

It is very interesting that  $D$  is negative for Zn compounds but is positive for Cd compounds. There are two different mechanisms<sup>14</sup> contributing to the  $D$  parameter. One involves the spin orbit interaction to second order and the axial field of a single  $d$ -electron and the cubic field to fourth order. The other mechanism mixes some  $3d^4 4s$  configuration with  $3d^5$  configuration. These mechanisms give rise to the expression

$$D = D_1 + D_2 = a_1 \frac{\langle r^2 \rangle}{R^3} + a_2 \left( \frac{\langle r^2 \rangle}{R^3} \right)^2 \quad (62)$$

where  $a_1$  and  $a_2$  are constants depending on  $\xi$ , the spin orbit coupling factor, and the difference of  $Mn^{++}$  orbital energy levels. According to Watanabe,<sup>14</sup>  $D_1$  is more pronounced than  $D_2$ ; therefore we can assume that in an ionic picture, the D parameter in different compounds varies as  $R^{-3}$  (R is inter-ionic distance) provided  $\langle r^2 \rangle$  remains the same. In Table III the values of  $R_1$  and  $R_2$  (Fig. 5) are given. A comparison of D values for  $Mn^{++}$  in ZnO, ZnS, and ZnSe (Table II) with the theoretical values obtained from Eq. (62) and Table III reveals that

$$\left( \frac{D_{ZnO}}{D_{ZnS}} \right)_T = 1.7 \quad , \quad \left( \frac{D_{ZnO}}{D_{ZnS}} \right)_E = 2 \quad (63)$$

and

$$\left( \frac{D_{ZnO}}{D_{ZnSe}} \right)_T = 2 \quad , \quad \left( \frac{D_{ZnO}}{D_{ZnSe}} \right)_E = 0.5 \quad (64)$$

where E and T stand for experimental and theoretical respectively. It is evident that though an ionic model for ZnO and ZnS gives a satisfactory result [Eq. (63)], it fails to account for the large value of D in ZnSe. This discrepancy is also present in CdS and CdSe. Therefore it is necessary to take the effect of covalency into account. The factor D can be expressed as a function of degrees  $\lambda_i$  of covalency and overlapping integrals  $S_i$  as follows:<sup>15</sup>

$$D = - 5.05 \Delta \text{ cm}^{-1}, \quad (65)$$

where

$$\Delta = (S'^2 - S^2) - (\lambda'^2 - \lambda^2), \quad (66)$$

$$S_i = \int \phi_{3do} \phi_{10} d\tau, \quad (67)$$

$$\lambda_i = (\phi_i - N\phi_{npo}) / N\phi_{3do}. \quad (68)$$

TABLE III

CRYSTALLINE PARAMETERS OF A<sub>II</sub> B<sub>VI</sub> COMPOUNDS [(R-x) = R(A<sup>0</sup>)]

Crystal	a <sub>0</sub> (A <sup>0</sup> )	c(A <sup>0</sup> )	c/a <sub>0</sub>	R <sub>1</sub> (A <sup>0</sup> )	R <sub>2</sub> (A <sup>0</sup> )	Ref.
ZnO	3.2426	5.1948	1.603	1.95	1.98	a
ZnS	3.811	6.234	1.636	2.33	2.33	a
ZnSe	3.98	6.55	1.645	2.45	-	b
CdS	4.131	6.691	1.619	2.51	2.53	a
CdSe	4.30	7.02	1.632	2.63	2.64	a

References: a. Wyckoff's Crystalline Structure.  
 b. Crystallography 5, 364 (1960).

$\phi_{3do}$  and  $\phi_{npo}$  denote the wave functions corresponding to the 3rd and the np electrons of Mn<sup>++</sup> and ligand with  $J_Z = 0$ . It is obvious that n has the values 2,3,4, and 5 for the ligands O, S, Se, and Te respectively.

Considering Fig. 7, one finds that

$$\frac{c}{a} = [a^2 - \kappa^2]^{1/2}; \quad \kappa^2 = \frac{4}{9}(a^2 - a^2/4) = a^2/3, \quad (69)$$

$$\frac{c}{2} = [2a^2/3]^{1/2} \quad \text{or} \quad c = 2a\sqrt{2/3},$$



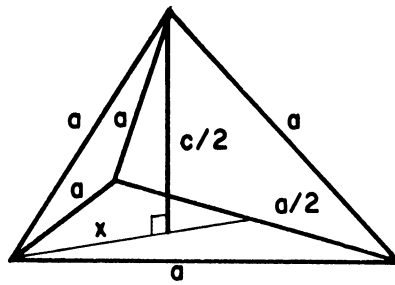


Fig. 7. Ideal hexagonal packing.

and

$$\frac{c}{a} = (8/3)^{1/2} = 1.6327 = 1.63.$$

Comparing Eq. (69) with the  $c/a$  ratios obtained for  $Zn(O,S,Se)$  in Table III, one finds that in  $ZnO$  the tetrahedron of oxygen ions is squashed along the C-axis, whereas in  $ZnSe$  it is elongated along the C-axis as shown in Fig. 8. This indicates that in the case of  $ZnO$  the relation be-

tween the overlapping integrals  $S_I$ ,  $S_{II}$ ,  $S_{III}$ , and  $S_{IV}$  is

$$S_{IV} > S_I, S_{II} \text{ or } S_{III}, \quad (70)$$

whereas for ZnSe it is

$$S_{VI} < S_I, S_{II} \text{ or } S_{III}. \quad (71)$$

Assuming  $S_I = S_{II} = S_{III} = S$  and  $S_{IV} = S'$  and recalling Eqs. (65-66),

one obtains

$$S'^2(\text{ZnO}) > S^2(\text{ZnO}),$$

where

$$S'^2(\text{ZnS}) < S^2(\text{ZnS})$$

and

$$S'^2(\text{ZnSe}) < S^2(\text{ZnSe}).$$

Therefore the overlap model ( $\lambda' = 0$ ) gives a correct sign of  $D$  for ZnO but an incorrect sign for ZnS and ZnSe. Consequently we must invoke the covalent model ( $\lambda \neq 0$ ) for ZnS and ZnSe, so that

$$(S'^2 - S^2) - (\lambda'^2 - \lambda^2) > 0. \quad (72)$$

Equation (72) indicates that for ZnS and ZnSe, the covalency effect is more pronounced than overlapping, and that  $\lambda'^2 < \lambda^2$ . In the case of CdS and CdSe we expect that  $\lambda'^2 > \lambda^2$  because the  $c/a$  ratio for these compounds

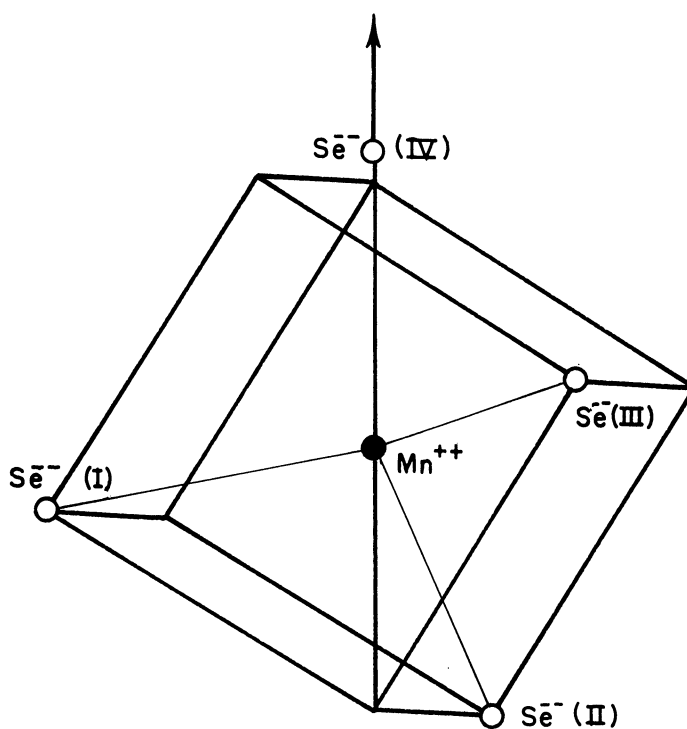


Fig. 8. A schematic representation of the surrounding Se ligands around the  $Mn^{++}$  ion in  $ZnSe:Mn$ .

(Table III) is less than 1.633. Therefore, according to this model we expect

$$D(CdS, CdSe) = -5.05[(S'^2 - S^2) - (\lambda'^2 - \lambda^2)] > 0. \quad (73)$$

Experimental results (Table III) confirm this prediction for the D value of  $Mn^{++}$  in CdS and CdSe. Further investigations regarding S and  $\lambda$  coefficients and their explicit dependence on the one-electron wave functions are under consideration. Until such relations are established, the only conclusion that can be drawn is that in the selenides of Zn and Cd

the covalency effects play a major role, whereas in their oxides the ionicity is more pronounced.

## REFERENCES

1. C. Kikuchi and G. H. Azarbayejani, J. Phys. Soc. Japan 17, Suppl. B-1, 453, (1962).
2. C. Kikuchi et al., The University of Michigan, Report 04275-2-F, Pt. III, (1963).
3. H. Watanabe, Prog. Theor. Phys. (Kyoto) 18, 405 (1957).
4. S. Slicker, J. Appl. Phys. 31, 1165 (1960).
5. Cuceaneau, Crystallography 5, 364 (1960).
6. R. H. Bube, Phys. Rev. 110, 1040 (1958).
7. Carl J. Ballhausen, Ligand Field Theory, McGraw-Hill (1962).
8. E. P. Wigner, Group Theory, Univ. of Calif., Los Alamos Scientific Laboratory (1959), p. 166.
9. B. Bleaney and W. H. Stevens, Repts. Prog. Phys. 16, 108 (1953).
10. C. Kikuchi and L. M. Matarrese, J. Chem. Phys. 33, 601 (1960).
11. G. Racah, Phys. Rev. 62, 438 (1942).
12. R. de L. Kronig and C. J. Bouwkamp, Physica 6, 290 (1939).
13. Reuben S. Title, Phys. Rev. 130, 17 (1963).
14. M. H. L. Pryce, Nuovo Cimento 6, Suppl., 843 (1957).
15. Jun Kondo, Prog. Theor. Phys. 23, 106 (1960).

UNIVERSITY OF MICHIGAN



3 9015 02227 0824